# Supplemental Material

## Immunothrombotic dysregulation in COVID-19 pneumonia is associated with respiratory failure and coagulopathy

Leo Nicolai[1,2,#,*], Alexander Leunig[1,2,#], Sophia Brambs[1], Rainer Kaiser[1,2], Tobias Weinberger[1,2], Michael Weigand[3], Maximilian Muenchhoff[4,5], Johannes C. Hellmuth[6,7], Stephan Ledderose[8], Heiko Schulz[8], Clemens Scherer[1,2], Martina Rudelius[8], Michael Zoller[9], Dominik Höchter[9], Oliver Keppler[4,5], Daniel Teupser[3], Bernhard Zwißler[9], Michael von Bergwelt-Baildon[6,7], Stefan Kääb[1,2], Steffen Massberg[1,2], Kami Pekayvaz[1,2,§,*] & Konstantin Stark[1,2,§]

[1] Medizinische Klinik und Poliklinik I, University Hospital Ludwig-Maximilian-University Munich, Munich, Germany
[2] DZHK (German Centre for Cardiovascular Research), partner site Munich Heart Alliance, 80802 Munich, Germany
[3] Institute of Laboratory Medicine, University Hospital Ludwig-Maximilian-University Munich, Munich, Germany
[4] Virology, Max von Pettenkofer Institute, Ludwig-Maximilian-University Munich, Munich, Germany
[5] German Center for Infection Research (DZIF), Partner Site Munich, Munich, Germany
[6] Medizinische Klinik und Poliklinik III, University Hospital Ludwig-Maximilian-University Munich, Munich, Germany
[7] German Cancer Consortium (DKTK), Munich, Bavaria 81377, Germany
[8] Institute of Pathology, Ludwig-Maximilian-University, Munich, Germany
[9] Department of Anesthesiology, University Hospital Ludwig-Maximilian-University Munich, Munich, Germany

[#] contributed equally
[§] contributed equally
[*] correspondence to: leo.nicolai@med.uni-muenchen.de and kami.pekayvaz@med.uni-muenchen.de

# Supplemental Figures and Figure Legends I – VIII:

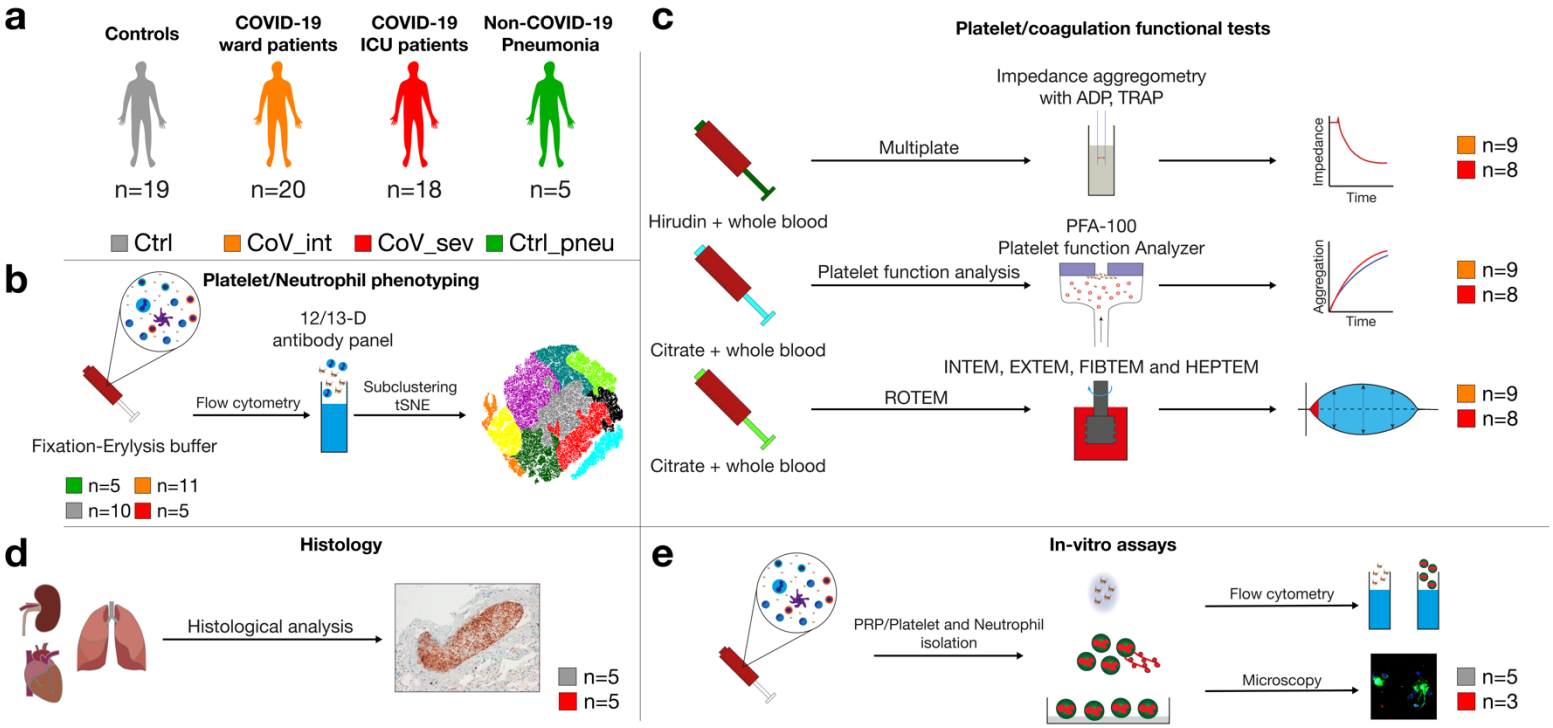


**Supplemental Figure I | Cohort and analysis strategy in COVID-19 patients. a,** Top left: Schematic group characteristics and number of patients per group for each experiment. **b,** Middle left: Analysis process for surface marker expression of platelets and neutrophils. Whole blood from patients was fixed, lysed and stained. After flow cytometry unsupervised clustering was performed. Number of patients for this analysis is shown below. **c,** Upper right: Illustration of tests of platelet and coagulation function. Whole blood was drawn into either hirudin or citrate vials and processed for each analysis. Number of patients for this analysis is shown on the right. **d,** Lower left: Illustration of histological analysis. **e,** Lower right: Illustration of performed *in vitro* assays. PRP, platelets and neutrophils were isolated from patient or control blood and analyzed after activation or fixation with flow cytometry or histology.

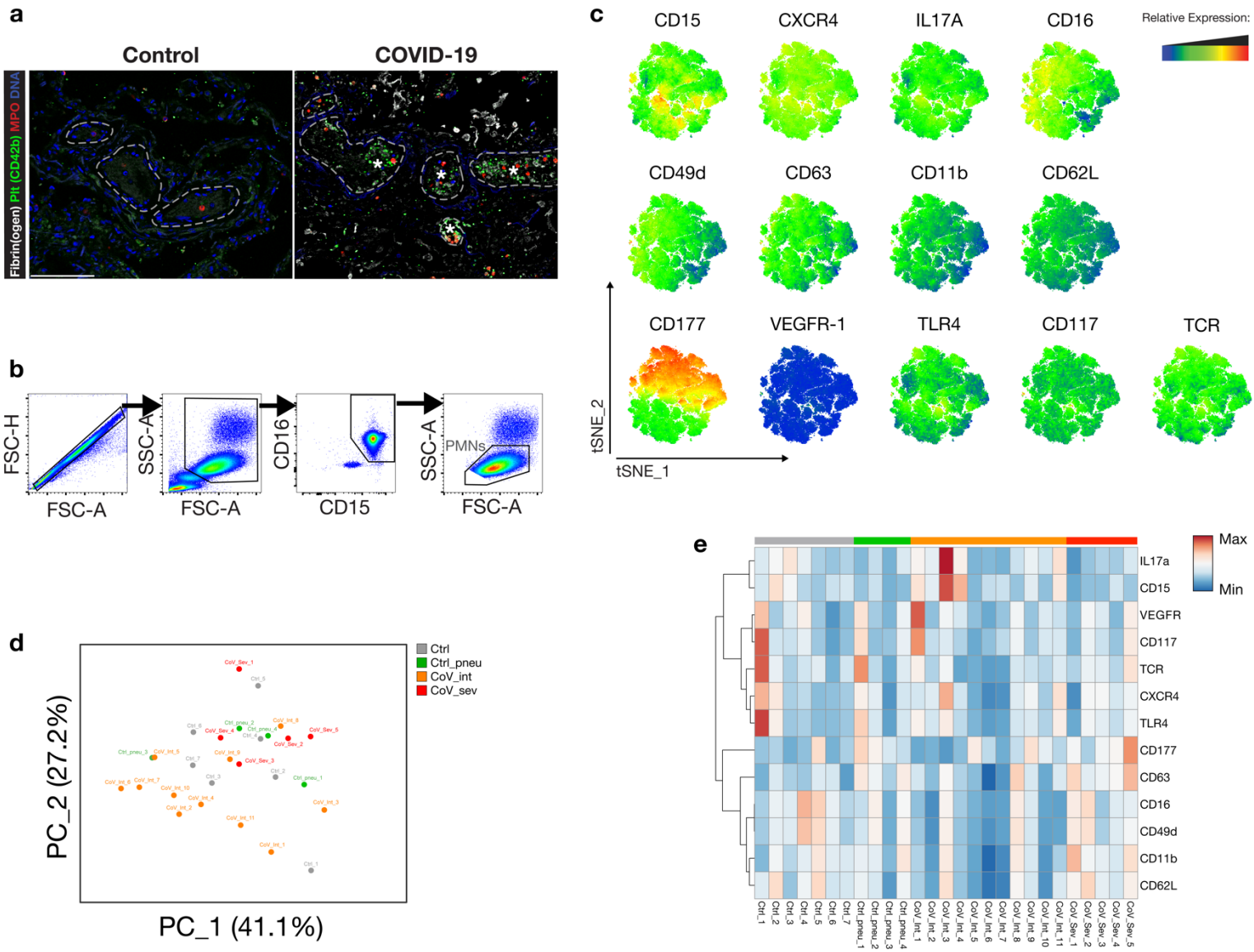


**Supplemental Figure II | Neutrophil gating strategy and in-depth analysis of neutrophil surface marker clustering. a,** Associated with Fig. 1f: Representative micrographs of immunofluorescence stainings for immunothrombosis in COVID-19 and control lung autopsy specimens. Stars: Intravascular areas with immunothrombosis. Scale bar: 100 µm, dashed lines indicate larger vessel borders. **b,** Gating strategy to identify the neutrophil (PMN) population. **c,** Plot of the median relative expression of neutrophil surface markers from the t-SNE analysis of Figure 2c-d. **d,** Principal component (PC) analysis of each patient's neutrophil surface marker expression (MFI). Patient IDs are displayed next to the data points. The percentage of variance explained by each principal component is stated in brackets. **e,** Heatmap of relative surface marker expression by patient. Patients are clustered into the respective groups. Plots d-e were generated using the ClustVis algorithm (Methods).

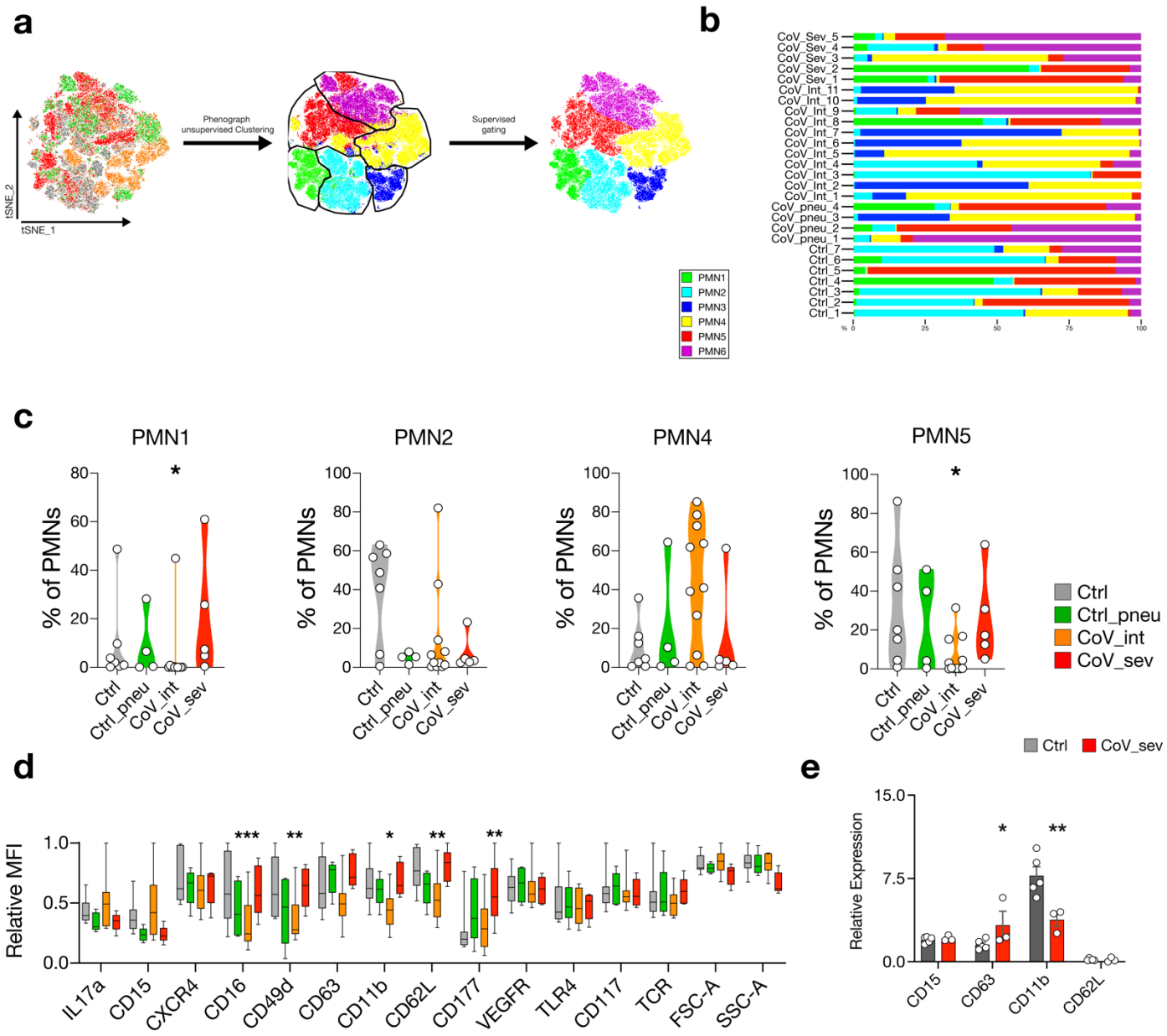


**Supplemental Figure III | Subclustering strategy, subcluster distribution of neutrophils and global expression of neutrophil surface markers. a,** Analysis strategy for neutrophil subpopulations. The t-SNE was subclustered with the Phenograph algorithm (nearest neighbors k=20). After unsupervised clustering, Phenograph clusters that matched in MFI values were merged and the subpopulations were gated manually on the basis of the Phenograph clustering. **b,** Percentage of neutrophils for the patients in each subcluster. Subclusters are denoted with the same colors as in a**. c,** Percentage of total neutrophils (PMN) of each patient that are in this subcluster are shown in violin plots. Percentages neutrophils in each subcluster are shown in gray above the heatmap. n=7 Ctrl, n=4 Ctrl_pneu, n=11 CoV_int, n=5 CoV_sev. For each subcluster population a Kruskal-Wallis test was performed, with a post hoc Dunn`s multiple comparison test. **d,** Relative neutrophil surface marker expression to maximum expression (shown as MFI), as well as mean FSC-A and SSC-A by group shown as box & whiskers plot (median, min to max) in arbitrary units (A.U.). n=10 Ctrl, n=5 Ctrl_pneu, n=11 CoV_int, n=5 CoV_sev for each surface maker. Two-way ANOVA with post-hoc Dunnett's multiple comparisons test. **e,** Relative expression of neutrophil activation markers compared to baseline after PMA stimulation. e-f: Unpaired, two tailed t-tests, n=3 COVID-19 severe patients, n=5 controls. * p<0.05, ** p<0.01, ***p<0.001.

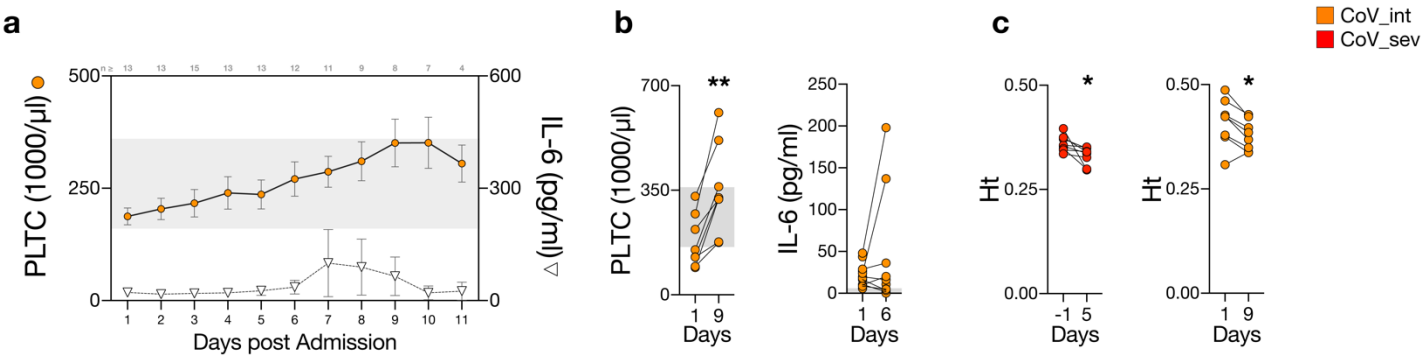


**Supplemental Figure IV | Platelet and IL-6 time-course of intermediate severity COVID-19 patients. a,** Time course of platelet count (orange spheres) and Interleukin-6 (IL-6, white triangles) of CoV_int patients normalized to the day of hospital admission. Number of patients for each time point shown above. Gray: reference range for platelet counts and IL-6 (PLTC 160-360 x1000/µl, IL-6 <5.9 pg/ml). **b,** Changes in platelet count and IL-6 measurements over time (days) in CoV_int patients. Reference range for platelet counts in gray (160 to 360 x1000/µl). n=8 for PLTC, n=8 for IL-6, two-tailed paired t-test. **c,** Changes in hematocrit of CoV_int and CoV_sev over time (days). CoV_int n=8 CoV_sev n=8, two-tailed paired t-test. * $p<0.05$, ** $p<0.01$.

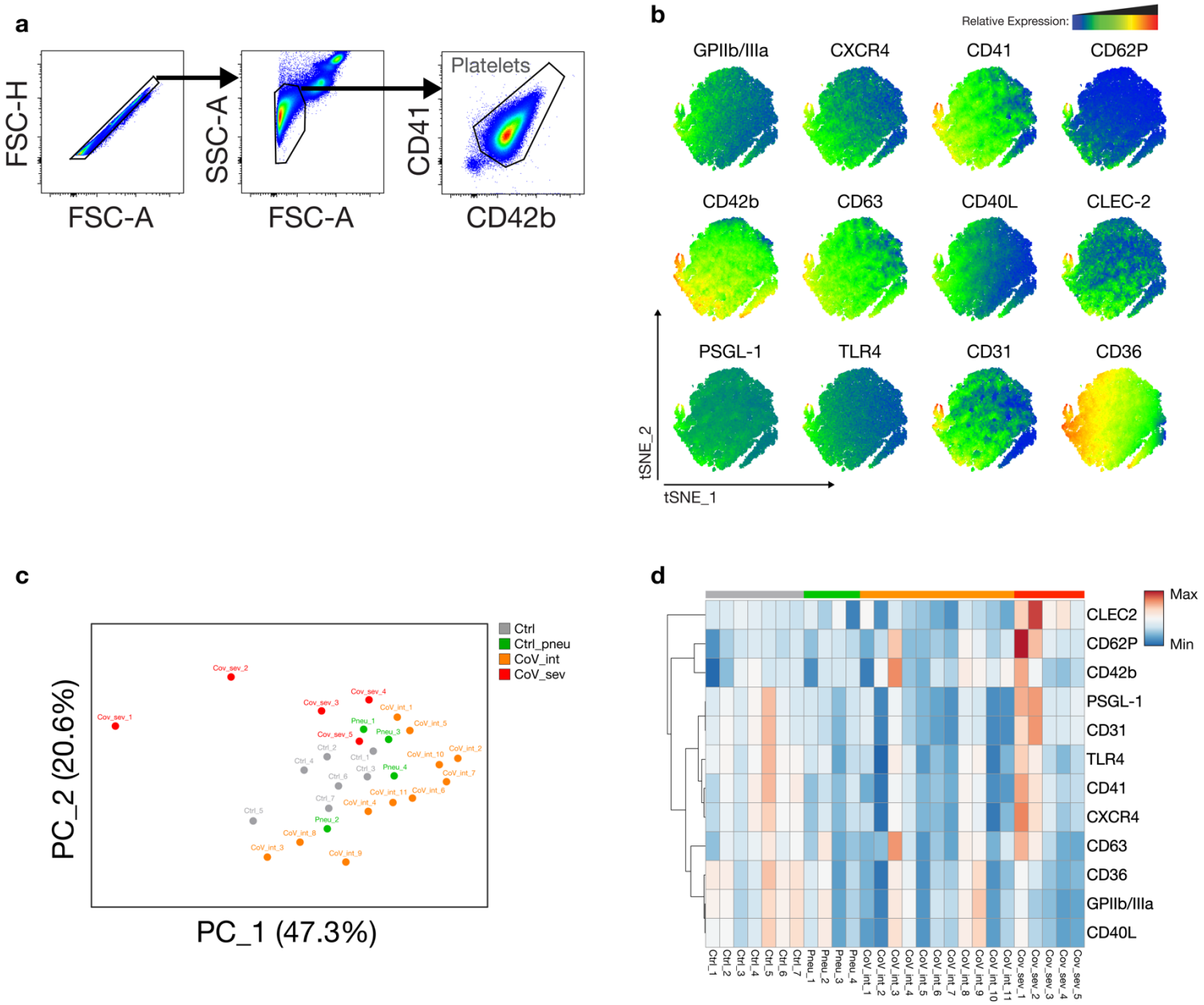


**Supplemental Figure V | Platelet gating strategy and in-depth analysis of platelet surface marker clustering.** **a,** Gating strategy to identify the platelet compartment. First, singlets were gated, then platelets by size and finally platelets were defined as CD42b$^{+}$ CD41$^{+}$. **b,** Plot of the median relative expression of platelet surface markers from the t-SNE analysis of Figure 2a-b. **c,** Principal component (PC) analysis of each patient's platelet surface marker value (MFI). Patient IDs are displayed next to the data points. The percentage of variance explained by each principal component is stated in brackets. **d,** Heatmap of relative platelet surface marker expression by patient. Patients are clustered into the respective groups. Plots c-d were generated using the ClustVis algorithm (Methods).

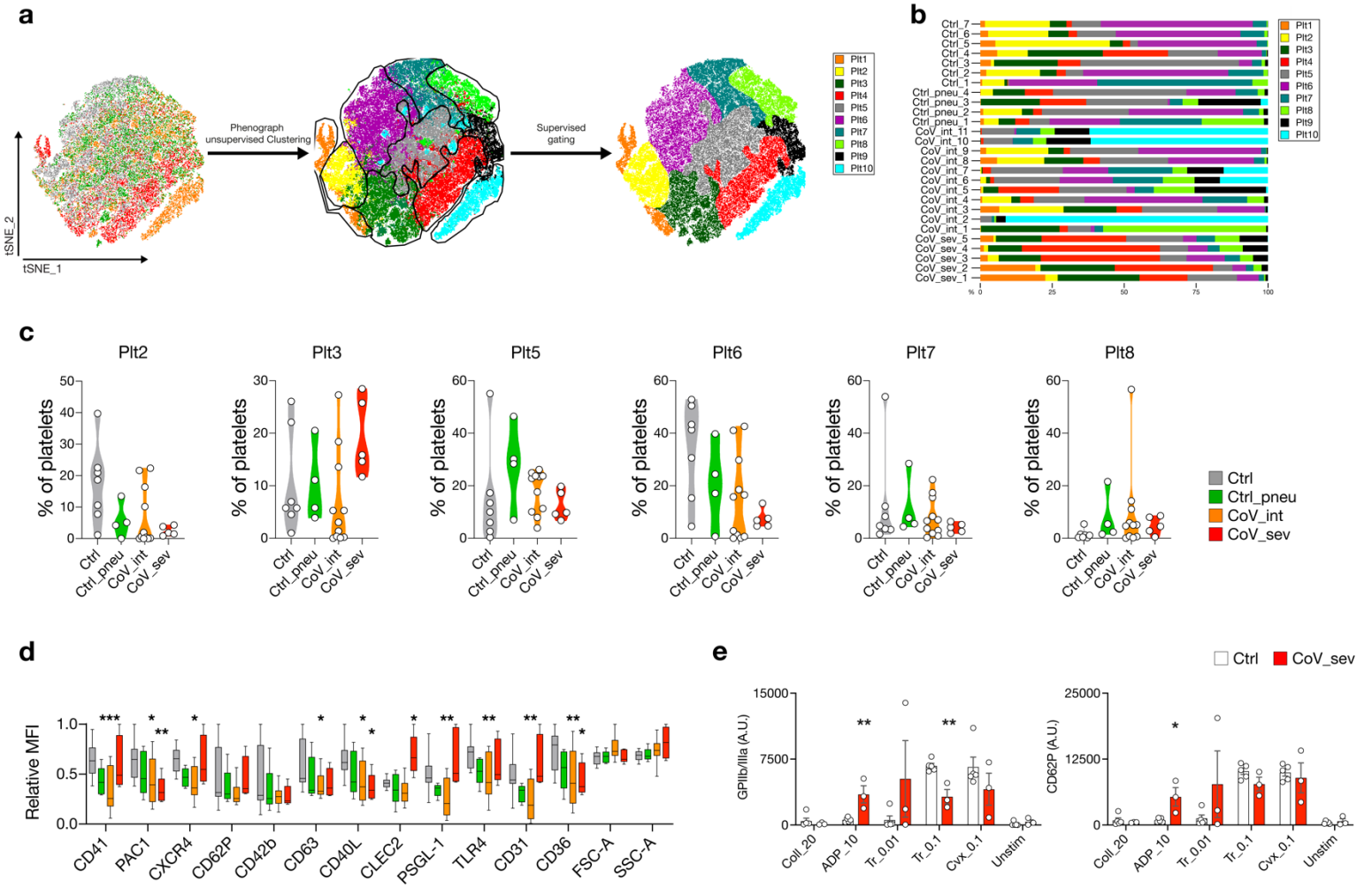


**Supplemental Figure VI | Subclustering strategy, subcluster distribution of platelets and global expression of platelet surface markers. a,** Analysis strategy for platelet subpopulations. The t-SNE was subclustered with the Phenograph algorithm (nearest neighbors k=20). After unsupervised clustering, Phenograph clusters that matched in MFI values were merged and the subpopulations were gated manually on the basis of the Phenograph clustering. **b,** Percentage of platelets for the patients in each subcluster. Subclusters are denoted with the same colors as in a. **c,** Percentage of total platelets of each patient that are in this subcluster (Plt) are shown in violin plots. Percentages platelets in each subcluster are shown in gray above the heatmap. n=7 Ctrl, n=4 Ctrl_pneu, n=11 CoV_int, n=5 CoV_sev. For each subcluster population a Kruskal-Wallis test was performed. **d,** Relative platelet surface marker expression to maximum expression (shown as MFI), as well as mean FSC-A and SSC-A by group shown as box & whiskers plot (median, min to max) in arbitrary units (A.U.). n=10 Ctrl, n=5 Ctrl_pneu, n=11 CoV_int, n=5 CoV_sev for each surface maker. Two-way ANOVA with post-hoc Dunnett's multiple comparisons test. **e,** Expression of GPIIb/IIIa and CD62P on platelets after activation by various stimuli, Unstim=control. Unpaired, two tailed t-tests, n=3 COVID-19 severe patients, n=5 controls. * p<0.05, ** p<0.01, ***p<0.001.

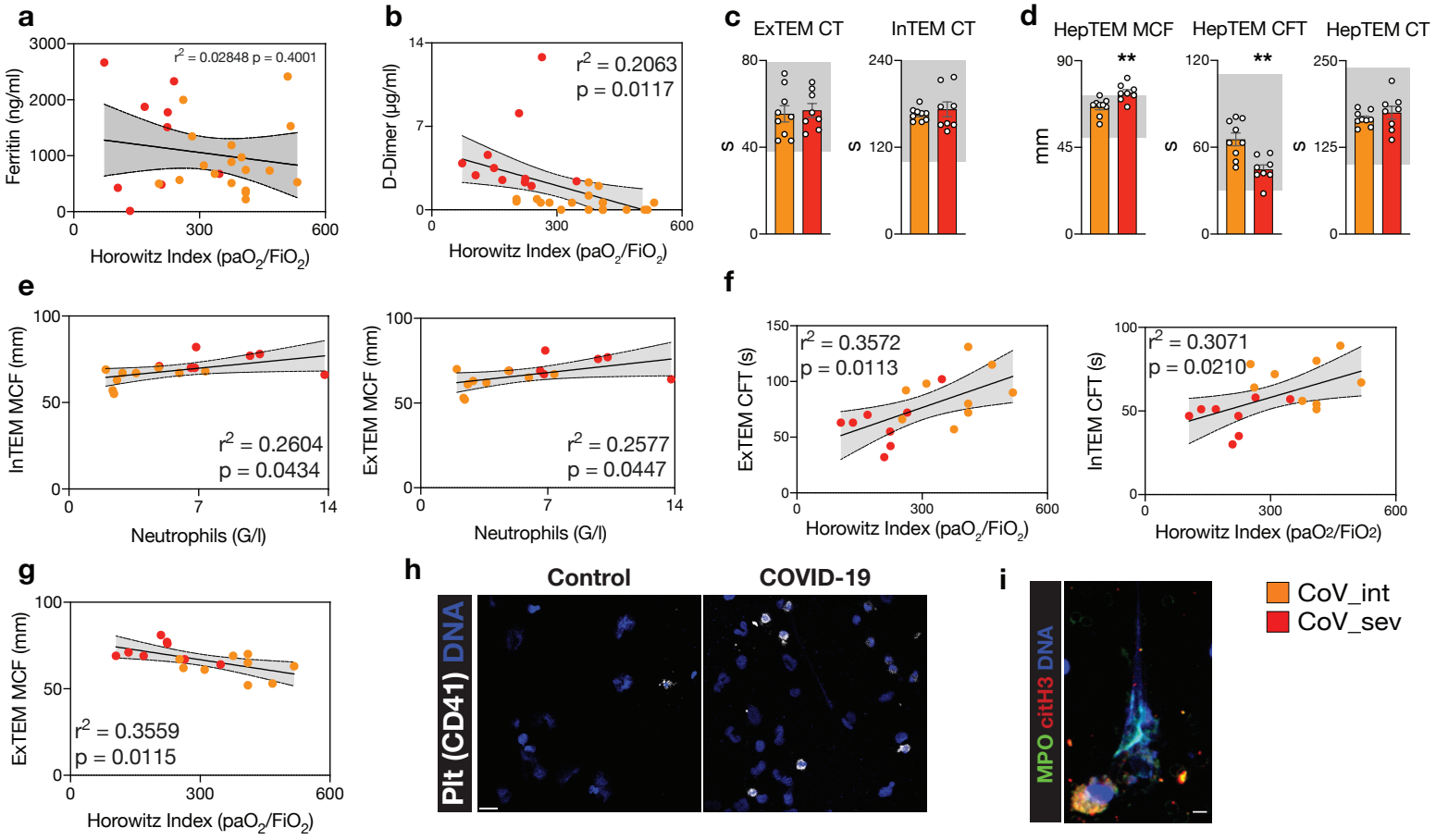


**Supplemental Figure VII | Linear regressions and rotational thrombelastometry data (InTEM, ExTEM and HepTEM). a-b,** Linear regression of ferritin and D-Dimer plasma level and Horowitz Index ($paO_2/FiO_2$) of COVID-19 patients. Ferritin n=18 CoV_int, n=9 CoV_sev, D-Dimer n=19 CoV_int. **c,** ExTEM and InTEM Clotting Time (CT) of COVID-19 patients. Reference ranges are shown in gray (ExTEM 38-79s, InTEM 100-240s). **d,** HepTEM Maximum Clot Firmness (MCF), Clot Formation Time (CFT) and Clotting Time (CT) of COVID-19 patients. Reference ranges are shown in gray (MCF 50-72mm, CFT 30-110s, CT 100-240s). n=9 CoV_int, n=8, Two-tailed unpaired Student's t-test. **e,** Linear regression of ExTEM and InTEM MCF with neutrophil count of COVID-19 patients. n=9 CoV_int, n=7 CoV_sev. **f,** Linear regression of ExTEM and InTEM CFT with Horowitz Index of COVID-19 patients. n=9 CoV_int, n=8 CoV_sev. **g,** Linear regression of ExTEM MCF and Horowitz Index of COVID-19 patients. n=9 CoV_int, n=8 CoV_sev. For all regressions: Black line represents best-fit line, gray area the 95% confidence interval. $r^2$ and p value (slope non-zero) are shown in the plots. **h,** Associated with Fig. 4m**:** Representative images of control or COVID-19 platelets associated with neutrophils. Scale bar: 20µm. **i,** Associated with Fig. 4n: representative micrograph of a NETing neutrophil superfused with COVID-19 PRP. Scale bar: 10 µm. ** p<0.01.

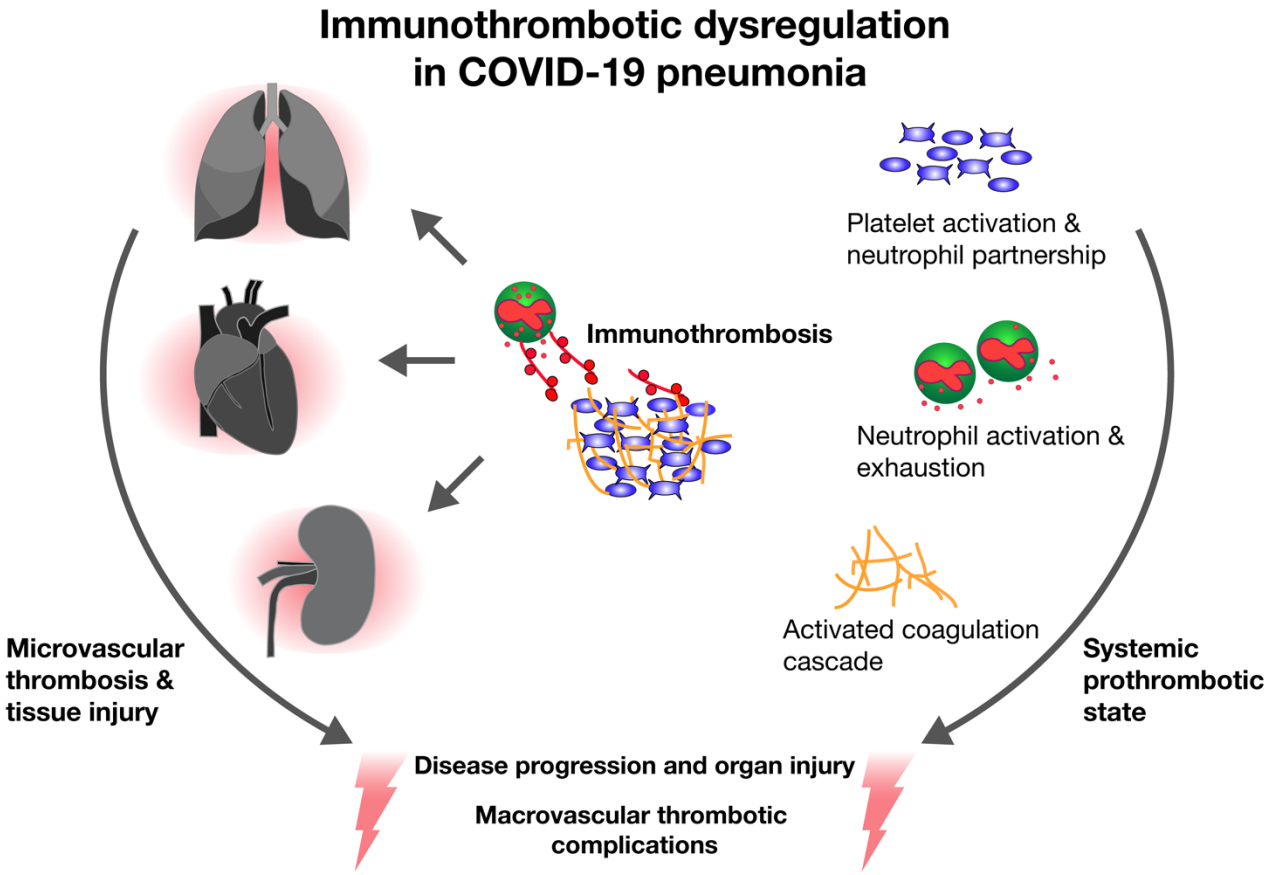


**Supplemental Figure VIII | Graphical abstract: Immunothrombotic dysregulation in COVID-19 pneumonia is associated with respiratory failure and coagulopathy.** Immunothrombosis is evident in the lung, heart and kidneys of COVID-19 patients, leading to microvascular thrombosis and subsequent tissue injury (left side). Platelet and neutrophil activation, neutrophil exhaustion, and an activated coagulation cascade driven by fibrinogen lead to a systemic prothrombotic state in COVID-19 patients that changes with disease severity (right side). All of the above contribute to disease progression in form of organ injury, as well as to the probability of macrovascular thrombotic complications in SARS-CoV-2 infection.

# Supplemental Tables I-III:

## Supplemental Table I | Additional clinical characteristics of patient cohorts:

| Cohort: | Control * | COVID-19_int | COVID-19_sev | Non COVID-19 Pneumonia ** |
|---|---|---|---|---|
| Patient count: | N = 10 | N = 20 | N = 11 | N = 5 |
| | | | | |
| **Demographics** | | | | |
| Age, Median Year [interquartile range [IQR]] | 61 [30-67] | 59 [51-70] | 56 [46-65] | 73 [44-86] |
| Male, n [%] | 7 [70] | 15 [75] | 9 [82] | 3 [60] |
| | | | | |
| **Underlying medical comorbidities** | | | | |
| Active cancer, n [%] | 0 [0] | 1 [5] | 0 [0] | 0 [0] |
| Immunocompromising conditions or treatments, n [%] | 0 [0] | 0 [0] | 0 [0] | 0 [0] |
| Atrial fibrillation / flutter, n [%] | 4 [40] | 1 [5] | 0 [0] | 3 [60] |
| Coronary artery disease, n [%] | 0 [0] | 1 [5] | 0 [0] | 1 [20] |
| Arterial hypertension, n [%] | 4 [40] | 9 [45] | 7 [64] | 4 [80] |
| Chronic kidney disease, n [%] | 1 [10] | 0 [0] | 0 [0] | 2 [40] |
| Diabetes mellitus, n [%] | 1 [10] | 3 [15] | 1 [9] | 2 [40] |
| Asthma / COPD / OSAS, n [%] | 1 [10] | 3 [15] | 1 [9] | 1 [20] |
| | | | | |
| **Pathogens** | | | | |
| SARS-CoV-2, n [% positive result] | --- | 20 [100] | 11 [100] | 0 [0] |
| Influenza, n [% positive result] | --- | 0 [0] † | 0 [0] †† | 0 [0] † |
| RSV, n [% positive result] | --- | 0 [0] † | 0 [0] ††† | 1 [20] † |
| Other identified pathogens (if determined), n [% positive result] | --- | 0 [0] | 0 [0] | 1 [20] # |
| Not further specified, n [%] | --- | 0 [0] | 0 [0] | 3 [60] ## |
| | | | | |
| **Clinical information at admission** | | | | |
| Fever, n [%] | 0 [0] | 19 [95] | 9 [82] § | 4 [80] |
| Cough, n [%] | 0 [0] | 18 [90] | 9 [82] § | 4 [80] |
| Shortness of breath, n [%] | 1 [10] | 10 [50] | 6 [55] § | 1 [20] |
| | | | | |
| **Clinical information during enrollment into the study** | | | | |
| Invasive ventillation, n [%] | 0 [0] | 0 [0] | 11 [100] | 1 [20] |
| FiO2, Median [IQR] | 21 [21-23] | 21 [21-28] | 43 [35-55] | 28 [25-59] |
| Horowitz index, Median [IQR] | 574 [359-690] | 388 [289-453] | 197 [134-223] | 307 [202-358] |
| Dialysis, n [%] | 0 [0] | 0 [0] | 1 [9] | 0 [0] |
| Catecholamine requirement, n [%] | 0 [0] | 0 [0] | 11 [100] | 1 [20] |
| ECMO requirement, n [%] | 0 [0] | 0 [0] | 0 [0] | 0 [0] |
| Signs of deep vein thrombosis or pulmonary embolism, n [%] | 0 [0] | 0 [0] | 0 [0] | 0 [0] |
| | | | | |
| **Main blood values during enrollment to the study** | | | | |
| CRP (mg/dl, ref.: ≤ 0,5), Median [IQR] | --- | 2.3 [0.5-7.3] | 14 [10-25] | 8.2 [5.7-17.9] |
| Creatinine (mg/dl, ref.: 0.5-1), Median [IQR] | --- | 0.8 [0.7-0.9] | 1.2 [0.7-1.9] | 1.0 [0.8-2.0] |
| GOT (U/l, ref.: ≤34), Median [IQR] | --- | 37 [28-57] | 52 [41-68] | 28 [24-48] |
| | | | | |
| **Main cell counts during enrollment to the study** | | | | |
| White blood cells (x1000/µl, ref.: 4-10,4), Median [IQR] | 6.7 [4.8-7.4] | 5.0 [3.8-6.6] | 10.4 [7.4-15.4] | 9.1 [7.1-11.7] |
| | | | | |
| **Radiological findings** | | | | |
| Chest CT, n [%] | --- | 20 [100] | 10 [91] | 4 [80] |
| Bipulmonary infiltrates, n [%] | --- | 17 [85] | 10 [91] | 3 [60] |
| Ground glass opacities, n [%] | --- | 19 [95] | 8 [73] | 2 [40] |
| | | | | |
| **Anticoagulation** | | | | |
| Enoxaparin s.c., n [%] §§ | 0 [0] | 15 [75] | 0 [0] | 0 [0] |
| Unfractionated heparin i.v., n [%] §§ | 0 [0] | 0 [0] | 11 [100] | 1 [20] |
| Apixaban p.o., n [%] | 4 [40] | 0 [0] | 0 [0] | 1 [20] |
| Phenprocoumon p.o., n [%] | 0 [0] | 1 [5] | 0 [0] | 0 [0] |
| Rivaroxaban p.o., n [%] | 0 [0] | 0 [0] | 0 [0] | 1 [20] |
| No anticoagulation, n [%] | 6 [60] | 4 [20] | 0 [0] | 2 [40] |

* Control group enrolls healthy donors without signs of infection and patients hospitalized for reasons other than acute inflammatory conditions, matched for age and underlying comorbidities as possible

** Non COVID-19 pneumonia enrolls patients with radiological and clinical signs of pneumonia, which were tested negative for SARS-CoV-2

# Ascertained pathogen: Mycoplasma pneumoniae

## Clinically and radiologically ascertained, not further specified pneumonia

§ Presenting complaints at admission from 2 COVID-19_Sev patients were indistinct

† Unavailable influenza and RSV status of 1 patient

†† Unavailable influenza status of 3 patients

††† Unavailable RSV status of 5 patients

§§ For PFA-100®, Multiplate® and ROTEM® analyses only patients with enoxaparin or unfractionated heparin were included

SUPPLEMENTARY TABLE 1: Additional clinical characteristics of patient cohorts

**Supplemental Table II | Neutrophil phenotyping panel:**

| Color | Antigen | Company | Cat. Number |
|---|---|---|---|
| BV650 | CD63 | Biolegend | 353026 |
| FITC | CD177 | Biolegend | 315804 |
| PE | VEGFR-1 (FLT-1) | Miltenyi | 130-124-438 |
| PERCP-Cy5.5 | TCR alpha/beta | Biolegend | 306724 |
| APC | CD15 | Biolegend | 301908 |
| APC-Cy7 | CD184 (CXCR4) | Biolegend | 306528 |
| BV 605 | CD49d | Biolegend | 304324 |
| BV786 | CD62L | Biolegend | 304830 |
| BV510 | CD16 | Biolegend | 302048 |
| BV 711 | CD11b | Biolegend | 301344 |
| AF 700 | IL-17A | Biolegend | 512318 |
| PE-Dazzle | CD117 | Biolegend | 313226 |
| PE-Cy7 | CD284 (TLR-4) | Thermo Fisher | 25-9917-42 |

**Supplemental Table III | Platelet phenotyping panel:**

| Color | Antigen | Company | Cat. Number |
|---|---|---|---|
| BV650 | CD63 | Biolegend | 353026 |
| FITC | CLEC-2 | Biolegend | 372007 |
| PE | CD162/PSGL1 | Biolegend | 328805 |
| PERCP-Cy5.5 | CD36 | Biolegend | 336223 |
| AF 647 | PAC-1 | Biolegend | 362806 |
| APC-Cy7 | CD184 (CXCR4) | Biolegend | 306513 |
| BV510 | CD42b | Biolegend | 303933 |
| BV 711 | CD154 (CD40L) | Biolegend | 310837 |
| AF 700 | CD41 | Biolegend | 303727 |
| BV421 | CD62P | Biolegend | 304925 |
| PE-Dazzle | CD31 (PECAM) | Biolegend | 303129 |
| PE-Cy7 | CD284 (TLR4) | Invitrogen | 25-9917-42 |